ELSEVIER

Thermochimica Acta 336 (1999) 17–25

thermochimica acta

www.elsevier.com/locate/tca

Thermal and spectroscopic studies of polymorphic transitions of zirconia during calcination of sulfated and phosphated $Zr(OH)_4$ precursors of solid acid catalysts

A.A.M. Ali, M.I. Zaki*

Chemistry Department, Faculty of Science, Kuwait University, P.O. Box 5969, Safat 13060, Kuwait

Received 11 February 1999; received in revised form 18 May 1999; accepted 19 May 1999

Abstract

Zirconia, ZrO_2, was synthesized by calcination of pure, sulfate-impregnated, and phosphate-impregnated $Zr(OH)_4$ at different temperatures in the range from 600 to 1100°C for 5 h. Weight variant and invariant processes involved were monitored by thermogravimetry, differential thermal analysis and differential scanning calorimetry. The bulk structure and phase composition of the zirconias thus produced were characterized by X-ray powder diffractometry, infrared absorption spectroscopy and Raman scattering spectroscopy. The results have been correlated, so as to reveal the influence of the sulfate and phosphate additives on the zirconia polymorphic transitions as a function of temperature. Accordingly, phosphate species have been revealed to stabilize or influence stabilization of cubic-structured zirconia at temperatures as low as 600–900°C, where it is otherwise unstable. IR- and LRa-observed formation of $Zr_2P_2O_7$ species (cubic-structured) is suggested to act as seed species for the stabilized cubic structure of zirconia. An analogous stabilizing influence was revealed for sulfate species, however, toward cubic and/or tetragonal zirconia, and functions within the thermal stability range of the sulfate (i.e. up to 720°C).

Keywords: Zirconia; Zirconia polymorphism; Influence of sulfate additives; Influence of phosphate additives; Thermal and spectroscopic studies

1. Introduction

In compliance with environmental necessities [1], various types of acidic solid materials have been developed and subjected to a range of characterization studies. In particular, metal oxides, complex oxides, various types of zeolites including ZSM-5, heteropoly acids, inter-layer compounds, solid superacids (Nafion-H, complex metal halides, sulfated and phosphated oxides of titanium, zirconium and iron), metal phosphates, niobic acid, are most interesting materials ([2,3], and references therein). Amongst the solid acids and superacids reported, zirconia-based materials (particularly, SO_4^{2-}/ZrO_2, PO_4^{3-}/ZrO_2, and ZrP_2O_7) have been accorded the greatest share of studies reported [4].

In two recent reports [5,6], we have communicated results of characterization studies of surface and bulk properties of sulfated and phosphated zirconias. It has been suggested [5] that Brønsted acid generated on sulfated zirconias obtained by calcination at 600°C of appropriate precursors containing either zirconium

*Corresponding author. Tel.: +965-481-1188; fax: +965-481-6482

E-mail address: zaki@kuc01.kuniv.edu.kw (M.I. Zaki)

0040-6031/99/$ – see front matter
PII: S0040-6031(99)00113-6

oxide (ZrO_2) or hydroxide ($Zr(OH)_4$). In contrast, Brønsted acid sites were observed on phosphated zirconias only when $Zr(OH)_4$ was the precursor used [5,6]. These findings were in line with literature reports [7–11]. In an attempt to account for the surface behavior of phosphated zirconia derived from the hydroxide, reference has been made [6] to reports [7,11] relating the behavior to the bulk phase composition of the calcination product.

It is widely accepted that zirconia assumes a number of structural polymorphs at atmospheric pressure [12], the crystallographic [13,14], dynamic [15] and chemical [16] properties of which have been communicated. Three of these polymorphs are well established: monoclinic (m-ZrO_2; C_{2h}^5 ($P2_1/c$); $Z = 4$), tetragonal (*t*-ZrO_2; D_{4h}^{15} ($P4_2/nmc$); $Z = 2$) and cubic (*c*-ZrO_2; O_h^5 ($Fm3m$); $Z = 4$) zirconia. Orthorhombic zirconia (o-ZrO_2) has also been indexed [17], and found to be metastable under atmospheric pressure and transforms into m-ZrO_2 on heating above 300°C, or when ground in a mortar. Diagnostic X-ray diffraction patterns [13,18], Raman shifts [18–22] and infrared absorptions [20,23] have been determined and reported for each of the these polymorphs. However, a straightforward utilization of these reported data is hampered by the fact that each of these polymorphs of zirconia may exist in one, or more, of the following states: stable, strained (thermally or mechanically), metastable, or stabilized state [19,21].

High-temperature studies of the stable states of zirconia at atmospheric pressure [18,20–22,24–27] indicate that m-ZrO_2 is stable below 700°C, and transforms into t-ZrO_2 at 650–1100°C. On further heating up to 2000–2100°C, t-ZrO_2 is transformed into c-ZrO_2. The influence of heating–cooling cycles (at 25–1250°C) on infrared [22] and Raman [21,22] spectra have been examined, and found to reveal a thermal hysteresis (at 950–1150°C) in the transition to stable t-ZrO_2. Accordingly, a reversible transition to a different tetragonal modification (D_{2h} or C_{2v}; $Z = 4$) was suggested [22]. Smith and Newkirk [14], discussing a similar observation, excluded formation of such a different t-ZrO_2 phase, but confirmed the reversible m-ZrO_2 → t-ZrO_2 transition over a wider range of temperatures (750–1180°C).

Influence of foreign-ion additives on the polymorphism of zirconia has been examined. Accordingly, it has been realized that c-ZrO_2, which is only stable at ≥2000°C, could be stabilized at much lower temperatures (<1200°C) by minor additives of oxidic Ce^{4+} [28], Y^{3+} [24,27,29], Ca^{2+} [30] and Mg^{2+} [30] cations. To the best of our knowledge, analogous studies of bearings of anionic additives are hardly encountered in the literature. A recent report considering influence of anions (namely SO_4^{2-}) on zirconia [31], was focused only on the surface textural consequences.

Therefore, the present investigation was undertaken to characterize impacts of sulfate and phosphate anions on polymorphic transitions of zirconia during calcination of $(NH_4)_2SO_4/Zr(OH)_4$ and $(NH_4)_2HPO_4/Zr(OH)_4$. To accomplish this objective: (a) the calcination pathway up to 1100°C was probed by thermoanalytical techniques (TG, DTA and DSC) for the involved thermochemical events; and (b) products obtained at 600°, 900° and 1100°C were analyzed by X-ray powder diffractometry, and Fourier-transform infrared and laser Raman spectroscopies.

2. Experimental

2.1. Materials

A MEL (Manchester, UK) zirconium hydroxide, formally $Zr(OH)_4$, was found by ICP analysis (using a GBC Integra XM sequential inductively coupled plasma spectrometer) to assume the molecular formula of $Zr(OH)_4 \cdot H_2O$. The excess mole of water could be completely eliminated by drying at 80°C for 24 h. The dried hydroxide was wet-impregnated with aqueous solutions of $(NH_4)_2SO_4$ (Chemtal, UK), or $(NH_4)_2HPO_4$ (BDH, UK), by stirring a 6.5-g portion of the hydroxide in a 75-ml portion of the solution at ambient temperature for 30 min. Slurries thus obtained (denoted as SZrOH and PZrOH, respectively) were dried at 80°C for 24 h, and then calcined at 600°, 900° and 1100°C in a stream of 50 cm^3 air/min for 5 h. The calcination temperatures were chosen on the basis of thermal analysis results (see below), and the products are discerned below by an arabic number symbolizing the calcination temperature applied. Thus, SZrOH6 means the 600°C calcination product of the sulfate-impregnated hydroxide. Based on the concentration of the impregnating solution, the

calcination products should contain ≈5 wt% SO_4^{2-}, or PO_4^{3-}, species.

For control, a 6.5-g portion of the original hydroxide was similarly wet-treated, dried (denoted WZrOH) and calcined; however, in the absence of the sulfate or phosphate compounds. The calcination products are similarly discerned by the temperature-symbolizing number.

2.2. Thermal analyses

Thermogravimetry (TG), differential thermal analysis (DTA) and differential scanning calorimetry (DSC) were performed on heating, typically, a 10–15-mg portion of test material at 10°C/min and 50 cm^3 air/min, using a Shimadzu thermal system 50 equipped with a work station. Highly sintered α-Al_2O_3 (Shimadzu, Japan) was the thermally inert reference for DTA measurements, and the heat of transition (28.24 J/g) of pure indium (Johnson Mattey, UK) at 157°C was adopted for DSC calibration.

2.3. Spectroscopic analyses

X-ray powder diffractometry (XRD) was carried out (at $10<2\theta<80^\circ$ and room temperature) using a Siemens D5000 diffractometer, equipped with Ni-filtered CuK_α radiation ($\lambda = 1.5406$ Å). The diffractometer was operated with 1° diverging and receiving slits at 50 kV and 40 mA, and a continuous scan was carried out with a step size of 0.04° and a step time of 2.0 s. An on-line automatic search system (PDF Database) facilitated observed data match with JCPDS standards. Unit cell parameters were determined by a least-squares refinements carried out using a commercial data handling system (WIN Metric).

Fourier-transform laser Raman (LRa) spectra were taken from test materials, which were lightly compacted, at 200–3600 cm^{-1} and a resolution of 0.2 cm^{-1}, employing a Perkin–Elmer system 2000 Raman spectrometer (USA), equipped with a near-infrared diode pumped Nd:YAG laser (1.064 μm). The laser power at the test sample was in the range of 50–100 mW.

Fourier-transform infrared (IR) transmission spectra were taken from thin wafers of KBr-supported test materials (<1 wt%) at 400–4000 cm^{-1} and a resolution of 5.3 cm^{-1}, using a Bruker IFS-25 spectrophotometer (Germany).

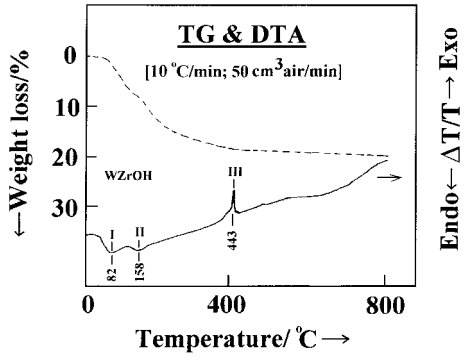

Fig. 1. TG and DTA curves for pure $Zr(OH)_4$.

3. Results

3.1. Thermo-analytical curves

TG and DTA curves (Fig. 1) monitor three thermochemical events (I–III) in the calcination course of WZrOH, the characteristics of which are set out in Table 1. Accordingly, it is obvious that conversion of WZrOH, i.e. pure, dried $Zr(OH)_4$, into ZrO_2 involves two weight loss (WL) events (I and II) and a weight invariant one (III). Event-I most probably involves the conversion of $Zr(OH)_4$ into $ZrO_2{\cdot}H_2O$, and event-II involves the dehydration of the product into ZrO_2 in two kinetically different processes. In view of the results and discussion presented by Mercera et al. [26], event-III may mark the crystallization into metastable t-ZrO_2 near 440°C.

TG and DTA curves for SZrOH (Fig. 2(A)) and PZrOH (Fig. 2(B)) indicate that the sulfate and phosphate additives do not significantly alter events I and II, which involves the hydroxide dehydration. However, they lead to disappearance of event-III and emergence of events-IV and -VI (in case of SZrOH) as well as event-V (in case of PZrOH). Events IV and V (Table 1) might be new, or additive-influenced modifications of the original event-III of the hydroxide. Event-VI, which moniters a minor WL-process commencing near 720°C (Table 1), is evidently sulfate-associated (Fig. 2(A)).

3.2. XRD patterns

XRD pattern (Fig. 3) obtained for WZrOH6 indicates, in line with the TG and DTA results (Fig. 1),

Table 1
Characteristics of thermochemical events monitored during the calcination pathway of pure, sulfated and phosphated $Zr(OH)_4$

Event	Characteristics				Remarks
	WL[a]/%	T_{max}[b]/°C	$\Delta T/T$	ΔH[c]/kJ mol^{-1}	
I	5–8	85	endo	7–11	
II	13	158–164	endo	7	invloves two kinetically different processes
III	—	443	exo	19	only observed for WZrOH
IV	—	509	exo	11	only observed for SZrOH
V	—	603	exo	5	only observed for PZrOH
VI	1.5	720[d]	—	—	only observed for SZrOH

[a] TG-deremined weight loss.
[b] Temperature at which rate of occurrence of the relevant event maximizes was determined by corresponding DTG curves (not shown).
[c] Enthalpy changes normalized per mole of ZrO_2 were determined by corresponding DSC curves (not shown).
[d] The temperature at which this particular event commences.

that the 600°C calcination of $Zr(OH)_4$ produces crystalline ZrO_2. The automatic matching of the results with the JCPDS standards attributes the diffraction peaks displayed to m- and c-ZrO_2 (and/or t-ZrO_2). The unit cell dimensions derived form the peaks assigned to m-ZrO_2 ($a = 5.314$ Å, $b = 5.215$ Å, $c = 5.150$ Å, $\alpha = 90.00°$, $\beta = 99.22°$ and $\gamma = 90.00°$) are very close to the standard data filed (JCPDS 37-1484) for monoclinic ZrO_2. However, the unit cell dimensions derived from the peaks assigned to c-and/or t-ZrO_2 ($a = b = 5.118$ Å, $c = 5.121\%$, $\alpha = \beta = \gamma = 90.00°$) are rather closer to those filed for face-centered cubic ZrO_2 (JCPDS 27-0997) than to tetragonal ZrO_2 (JCPDS 17-0923).

Comparing the above XRD pattern with those obtained for the 900° (WZrOH9) and 1100°C

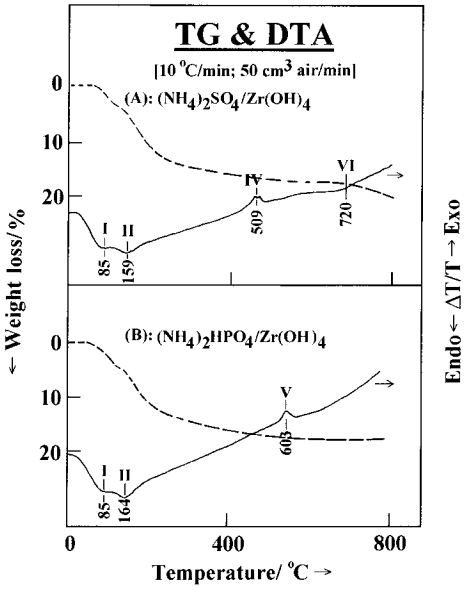

Fig. 2. TG and DTA curves for (A) sulfated and (B) phosphated $Zr(OH)_4$.

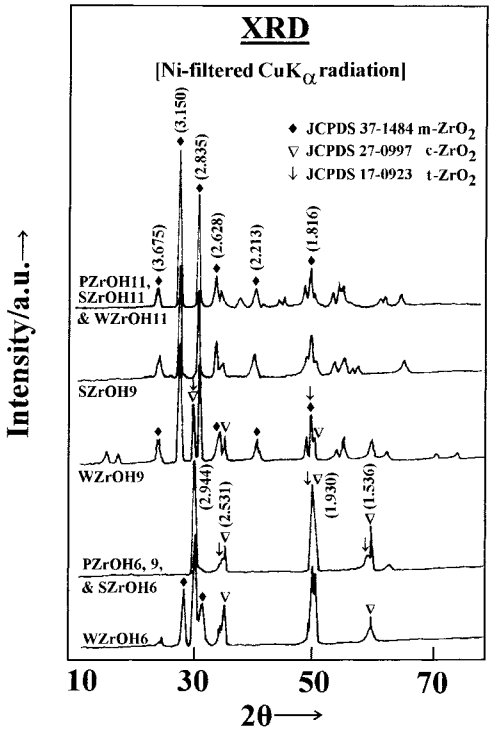

Fig. 3. X-ray powder diffractograms for the indicated calcination products of pure, sulfated and phosphated $Zr(OH)_4$ [values in parenthesis are for corresponding d-spacings in Ångstroms].

(WZrOH11) calcination products of $Zr(OH)_4$ (Fig. 3), one can easily realize intensification of the peaks due to m-$ZzrO_2$ at the expense of the other peaks of WZrOH9, till becoming dominant in the pattern of WZrOH11. In the presence of sulfate (SZrOH) and phosphate (PZrOH) additives, however, the m-ZrO_2 peaks are completely suppressed in the XRD patterns of SZrOH6 and PZrOH6, which are dominated by peaks due to c- and/or t-ZrO_2 (Fig. 3). The same only applies to PZrOH9, since for SZrOH9 the peaks of m-ZrO_2 are the dominant features in the respective XRD pattern (Fig. 3). Calcination products of SZrOH and PZrOH at 1100°C gave rise to very similar XRD patterns to that of WZrOH11, thus displaying dominantly characteristic peaks of m-ZrO_2.

The XRD results indeed relate the DTA-monitored events IV and V (Fig. 2, Table 1) to event-III (Fig. 1, Table 1). Accordingly, sulfate additives may be seen to retard the crystallization of zirconia (into cubic and tetragonal structures) to occur near 500°C, whereas phosphate additive to further the retardation to near 600°C.

3.3. IR spectra

IR spectra measured for the test materials are shown in Fig. 4. The spectra taken from the various calcination products (600–1100°C) of pure $Zr(OH)_4$ are dominated by absorptions (at 739, 576–580, 503–519, and 423–422 cm^{-1}) due to Zr–O bond vibrations assignable to m-ZrO_2 [5,6,20,22]. The better resolution and higher intensity of these bands in the spectra of the calcination products at ≥900°C are indicative of increasing purity and crystallinity of m-ZrO_2 with temperature. Thus, coexistence of the XRD-detected t-ZrO_2 in WZrOH6 is not visualized in the respective IR spectrum.

In accordance with XRD results (Fig. 3), the presence of sulfate and phosphate in the 600°C calcination products SZrOH6 and PZrOH6 modifies significantly the νZr–O spectral behavior at <900 cm^{-1}, and results in the manifestation of their respective S–O and P–O bond vibration absorptions at 950–1250 cm^{-1}. SZrOH6 displays an ill-defined, strong absorption due to Zr–O bond vibrations, only resolving two maxima at 589 and 496 cm^{-1}, in addition to the band structure (at 1248, 1142, 1075, 1044 and 1000 cm^{-1}) assignable to various modes of S–O

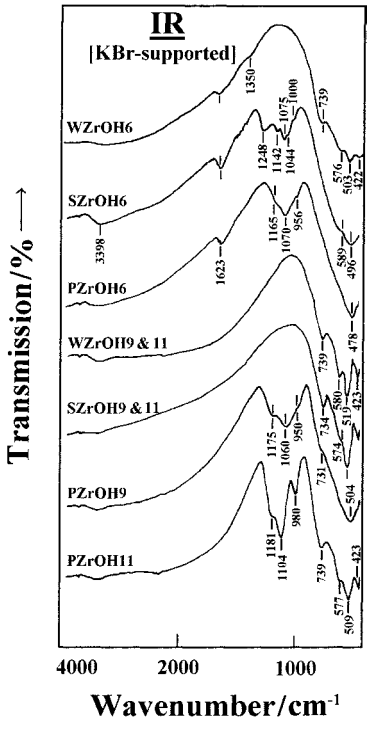

Fig. 4. FT-IR spectra for the indicated calcination products of pure, sulfated and phosphated $Zr(OH)_4$.

bond vibrations of differently structured sulfate species [32]. The display of two Zr–O bond absorptions only may account for the formation of more symmetric zirconia structures than m-ZrO_2. This can be fulfilled by the XRD-detected formation of c- and/or t-ZrO_2. These two bands are even merged into one strong, though still broad, band at 478 cm^{-1}, in the spectrum taken from PZrOH6. According to Phillippi and Mazdiyasni [20], the single band observed for PZrOH6 at 478 cm^{-1} arises from metastable c-ZrO_2, and the two bands observed at 589 and 496 cm^{-1} in the spectrum of SZrOH6 imply coexisting t-ZrO_2. IR spectrum of PZrOH6 shows moreover, three absorptions (at 1165, 1070 and 956 cm^{-1}) due to P–O bond vibrations of phosphate species [5,6,20].

Upon calcination at ≥900°C, the products SZrOH9 and SZrOH11 exhibit similar IR spectra, showing no absorptions (at 1000–1250 cm^{-1}) due to S–O bond vibrations. They show, however, the characteristic band structure of m-ZrO_2 at <900 cm^{-1}. The elimination of sulfate absorptions may be correlated with the TG-monitored WL event-VI for SZrOH, which com-

mences near 720°C (Fig. 2(A), Table 1). On the other hand, the product PZrOH9 maintains the same spectral features of PZrOH6 (Fig. 4), except for a large frequency shift of the 478 cm^{-1} band to occur at 503 cm^{-1} and the emergence of a shoulder at 731 cm^{-1}. These modifications may account for the formation of a minor proportion of m-ZrO_2. The higher calcination product PZrOH11 displays a spectrum monitoring some significant high-frequency shifts and relative intensity modifications in the phosphate band structure (Fig. 4), which were previously used [6,33] to evidence the polymerization of ortho-phosphate (PO_4^{3-}) into pyro-phosphate ($P_2O_7^{4-}$) species. It also monitors the characteristic band structure of m-ZrO_2.

3.4. LRa spectra

LRa spectra obtained for the 600°C calcination products are exhibited in Fig. 5, whereas those measured for the higher calcination products (at ≥900°C) are shown in Fig. 6. The peaks displayed for WZrOH6 could be attributed to coexisting m-ZrO_2 (diagnostic peaks at 638, 617, 559, 538, 502, 476, 382, 337, 307, 223 and 192 cm^{-1} [20,22]) and t-ZrO_2 (diagnostic peaks at 640, 615, 561, 536, 473, 380, 332, 263, 223 and 189 cm^{-1} [20,22]). As per the reference peak frequencies, it is obvious that the diagnostic LRa peaks for m- and t-ZrO_2 assume close frequency values, and these are, probably, the two weak peaks at 266 and 219 cm^{-1} that can be used to discern t- from m-ZrO_2. On the other hand, the two calcination products SZrOH6 and PZrOH6 exhibit similarly three major peaks at 641, 457 and 272 cm^{-1}, as well as two distinct shoulders at 310 and 190 cm^{-1}. These LRa peaks cannot be attributed to m-ZrO_2 (see above), though may conceal peaks due to t-ZrO_2. Therefore, they must be related to the more symmetric IR- (Fig. 4) and XRD-anticipated (Fig. 3) c-ZrO_2. Cubic zirconia has been shown to give rise to a single LRa peak at 490 cm^{-1} when in a metastable state, and to a set of five peaks (at 625, 480, 360, 250 and 150 cm^{-1}) when Y_2O_3-stabilized [20]. Thus, the present set of peaks may imply the formation of sulfate- and phosphate-stabilized c-ZrO_2 in SZrOH6 and PZrOH6,

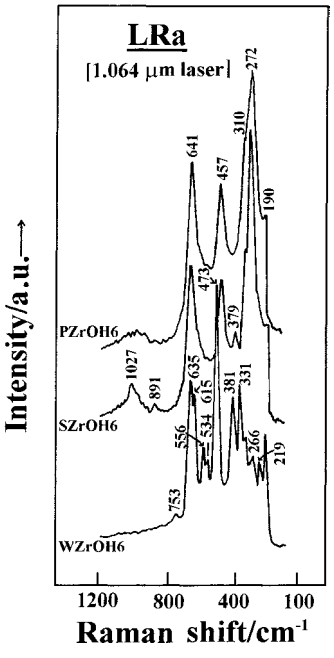

Fig. 5. FT-LRa spectra for the indicated calcination products of pure, sulfated and phosphated $Zr(OH)_4$.

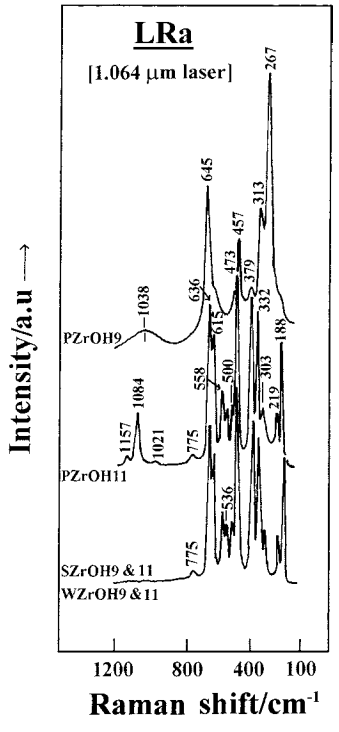

Fig. 6. FT-LRa spectra for the indicated calcination products of pure, sulfated and phosphated $Zr(OH)_4$.

respectively. It is worth noting, however, that the peak uniquely displayed for SZrOH6 at 379 cm^{-1} may indicate the presence of t-ZrO_2 and/or m-ZrO_2. Moreover, the weak peaks displayed for the latter material around 1027 and at 891 cm^{-1} are due to the sulfate species [5,6], whereas the broad peak, centred around 1027 cm^{-1} in the spectrum of PZrOH6, is associated with ortho-phosphate species [5,6].

The $\geq$900°C calcination products of WZrOH and SZrOH give rise to largely similar LRa spectra, only displaying the characteristic penks of m-ZrO_2 (see above). Thus, the sulfate peaks observed for SZrOH6 have been eliminated on heating at $\geq$900°C, as shown in the relevant IR spectra (Fig. 4). In contrast, the calcination product PZrOH9 maintains the spectral features exhibited by PZrOH6 (Fig. 5), which account for the presence of phosphate species and bulk composition of stabilized c-ZrO_2. The tiny peak observed for PZrOH9 at 379 cm^{-1} may mark the beginning of formation of m-ZrO_2. Increasing the calcination temperature up to 1100°C obviously improves the LRa peak structure of m-ZO_2 at the expense of that of c-ZrO_2, and the polymerization of orthophosphate species to give peaks (at 1157, 1084 and 1021 cm^{-1}) characteristic of pyro-phosphate species ($P_2O_7^{4-}$) [5,6] for PZrOH11.

4. Discussion

4.1. Zirconia polymorphism

The parent MEL $Zr(OH)_4$ has been found to assume the molecular formula $Zr(OH)_4 \cdot H_2O$ ($\approx ZrO_2 \cdot 3H_2O$). This finding is compatible with the uniquely high electron affinity and covalency of zirconium atoms [16] which urged Cotton and Wilkinson [34] to consider that $Zr(OH)_4$ was non-existent and was actually $ZrO_2 \cdot nH_2O$. On drying at 80°C, the excess mole of water is easily driven off, and the material assumes the stoichiometric composition $Zr(OH)_4$ ($=ZrO_2 \cdot 2H_2O$). On heating in air (calcination) it is dehydrated in two endothermic processes ($T_{max} = 85^\circ$ and 158°C) yielding non-crystalline zirconia near 400°C. As the temperature approaches 440°C, a glow release of heat ($\Delta H = -19$ kJ/mol$-ZrO_2$) DSC determined (Table 1). It marks the crystallization into metastable t-ZrO_2 with minority m-ZrO_2. The amount of heat determined is in good agreement with the values (16–19 kJ/mol) reported by Torralvo et al. [35], and smaller than that (28 kJ/mol) reported by Haberko et al. [36]. Keramidas and White [18] have attributed the formation of the otherwise unstable t-ZrO_2 at $\leq$600°C to a favourable atomic arrangement in the non-crystalline zirconia, and to the presence of minority intergrowths of m-ZrO_2.

According to Table 2, the 600°C calcination product of $Zr(OH)_4$, i.e. WZrOH6, essentially consists of metastable t-ZrO_2 and a minority of m-ZrO_2. On further heating of the hydroxide to 900°C, m-ZrO_2 is developed at the expense of the metastable t-ZrO_2 (Table 2). At 1100°C, m-ZrO_2 becomes the dominant polymorph of zirconia in the bulk composition of the calcination product (WZrOH11, Table 2). Hence, the polymorphic transitions of pure zirconia in the temperature range scanned essentially involves the conversion of metastable t-ZrO_2 into m-ZrO_2, which dominates at 1100°C.

Table 2
Zirconia polymorphic transitions as a function of calcination temperature (for 5 h) and sulfate and phosphate additives

Calcination temperature/°C	Precursor			Remarks
	WZrOH	SZrOH	PZrOH	
600	t-ZrO_2(j[b]) and m-ZrO_2(m[c])	c- and/or t-ZrO_2(d[a])	c-ZrO_2(d[a])	t-ZrO_2 is metastable, and c-ZrO_2 is stabilized
900	m-ZrO_2(j[b]) and t-ZrO_2 (m[c])	m-ZrO_2(d[a])	c-ZrO_2(d[a]) and m-ZrO_2(t[d])	m-ZrO_2 is stable
1100	m-ZrO_2(d[a])	m-ZrO_2(d[a])	m-ZrO_2(d[a])	m-ZrO_2 is stable

[a] Dominant.
[b] Major.
[c] Minor.
[d] Trace.

4.2. Influence of the salt additives

Table 2 indicates that phosphate additive could stabilize, or influence the stabilization of c-ZrO_2 at the expense of t- and m-ZrO_2 at a temperature as low as 600°C. A similar effect has been observed for oxidic additives of Ce^{4+} [28], Y^{3+} [24,27,29], Ca^{2+} [30] and Mg^{2+} [30]. The influence of phosphate has been maintained up to 900°C, and may be correlated with the IR- (Fig. 4) and LRa-observed (Fig. 6) formation of cubic-structured $Zr_2P_2O_7$ [37] during calcination up to 1100°C. On the other hand, the influence of sulfate additive is also stabilizing, though it is not definite whether it stabilizes t-ZrO_2 or both t-ZrO_2 and c-ZrO_2. It ceases near 700°C as a result of the sulfate thermal decomposition (Fig. 2(A) and Figs. 4 and 6). Consequently, the low-temperature sulfate-stabilized c- and/or t-ZrO_2 is transformed into m-ZrO_2 at $\geq$900°C (Table 2). Although pyro-phosphate species were still observed at 1100°C (Figs. 4 and 6), the stabilized c-ZrO_2 is transformed almost completely into m-ZrO_2 in the calcination product (PZrOH11) thus obtained.

5. Conclusion

Zirconia synthesized by calcination of pure $Zr(OH)_4$ is crystallized near 440°C into metastable tetragonal zirconia (t-ZrO_2) with minority monoclinic zirconia (m-ZrO_2). The t-ZrO_2 is transformed into m-ZrO_2 on increasing the calcination temperature up to 1100°C, where m-ZrO_2 dominates the bulk composition.

When derived from phosphated $Zr(OH)_4$, zirconia polymorphism is influenced to assume the cubic structure (c-ZrO_2) at 600–900°C, which transforms into m-ZrO_2 at 1100°C. The simultaneous polymerization of PO_4^{3-} monomers into cubic-structured pyro-phosphate ($P_2O_7^{4-}$) species is seen to seed the stabilized structure of c-ZrO_2.

Using sulfated $Zr(OH)_4$ as a precursor, results in stabilized c- and/or t-ZrO_2 at 600°C. The resulting bulk structure is transformed into m-ZrO_2 as the sulfate species are thermally eliminated at 700–900°C.

Acknowledgements

The analytical work involved in the present investigation was carried out at the Analytical Services Laboratory (Analab) of the Chemistry Department, which is supported by the general facility project SAF No. SLC 063 of Kuwait University. The technical assistance provided at Analab, and the permission granted by the Geology Department of the Faculty of Science to carry out the XRD measurements (SAF No. SLD 002), are highly appreciated.

References

[1] G. Ertl, H. Knözinger, J. Weitkamp (Eds.), Handbook of Heterogeneous Catalysis, vol. 4. Wiley–VCH, Weinheim, 1997. pp. 1559–1696.
[2] K. Tanabe (Ed.), A Special Double Issue Devoted to Advances in Acidic and Basic Solid Materials, Part 1: Acidic Solid Materials, Mater. Chem. Phys., vol. 17. 1987.
[3] G. Ertl, H. Knözinger, J. Weitkamp (Eds.), Handbook of Heterogeneous Catalysis, vol. 1. Wiley–VCH, Weinheim, 1997. pp. 118–412.
[4] K. Tanabe, H. Hattori. In: G. Ertl, H. Knözinger, J. Weitkamp (Eds.), Handbook of Heterogeneous Catalysis, vol. 1. Wiley–VCH, Weinheim, 1997. pp. 404–412.
[5] M.I. Zaki, A.A.M. Ali, Coll. Surf. 119 (1996) 39.
[6] A.A.M. Ali, M.I. Zaki, Coll. Surf., 139 (1998) 81.
[7] K. Arata, Adv. Catal. 37 (1990) 165.
[8] M. Waqif, J. Bachelier, O. Sauer, J.C. Lavalley, J. Mol. Catal. 72 (1992) 127.
[9] A. Corma, A. Martinez, C. Martinez, J. Catal. 149 (1994) 52.
[10] T. Riemer, D. Spielbauer, M. Hunger, G.A.H. Mekhemer, H. Knözinger, J. Chem. Soc., Chem. Commun., 1994. pp. 1181.
[11] D. Spielbauer, G.A.H. Mekhemer, T. Riemer, M.I. Zaki, H. Knözinger, J. Phys. Chem. 101 (1997) 4681.
[12] E.C. Subbarao, In: A.H. Heuer, L.W. Hobbs (Eds.), Advances in Ceramics, Vol. 3, Science and Technology of Zirconia, American Ceramic Society, Columbus, OH, 1981. pp. 1–24.
[13] J.D. McCullough, K.N. Trueblood, Acta Cryst. 12 (1959) 507.
[14] D.K. Smith, H.W. Newkirk, Acta Cryst. 18 (1965) 983.
[15] E. Anastassakis, B. Papanicolaou, I.M. Asher, J. Phys. Chem. Solids 36 (1975) 667.
[16] Shih-Ming Ho, Mater. Sci. Eng. 54 (1982) 23.
[17] R. Suyama, T. Ashida, S. Kume, J. Am. Ceram. Soc. 68 (1986) 314.
[18] V.G. Keramidas, W.B. White, J. Am. Ceram. Soc. 57 (1974) 22.
[19] D.P.C. Thackeray, Spectrochim. Acta 30A (1974) 549.
[20] C.M. Phillippi, K.S. Mazdiyasni, J. Am. Ceram. Soc. 54 (1971) 254.

[21] M. Ishigame, T. Sakurai, J. Am. Ceram. Soc. 60 (1977) 367.
[22] C.H. Perry, F. Lu, D.W. Liu, B. Alzyab, J. Raman Spectroscopy 21 (1990) 577.
[23] T. McDevitt, W.L. Baun, J. Am. Ceram. Soc. 47 (1964) 622.
[24] A. Feinberg, C.H. Perry, J. Phys. Chem. Solids 42 (1981) 513.
[25] J.C. Hamilton, A. Nagelberg, J. Am. Ceram. Soc. 67 (1984) 686.
[26] P.D.L. Mercera, J.G. Van Ommen, E.B.M. Doesburg, A.J. Burggraaf, J.R.H. Ross, Appl. Catal. 57 (1990) 127.
[27] C.H. Perry, D.W. Liu, J. Am. Ceram. Soc. 68 (1985) 184.
[28] P. Duwez, F. Odell, J. Am. Ceram. Soc. 33 (1950) 274.
[29] K.S. Mazdiyasni, C.T. Lynch, J.S. Smith II, J. Am. Ceram. Soc. 50 (1967) 532.
[30] P. Duwez, F. Odell, F.H. Brown Jr., J. Am. Ceram. Soc. 35 (1952) 107.
[31] S.R. Vaudagna, R.A. Comelli, N.S. Figoli, React. Kinet. Catal. Lett. 58 (1996) 111.
[32] E. Steger, W. Schmidt, Ber. Bunsenges. Phys. Chem. 68 (1964) 102.
[33] G. Busca, V. Lorenzelli, P. Galli, A.L. Ginestra, P. Patrono, J. Chem. Soc., Faraday Trans. I 83 (1987) 853.
[34] F.A. Cotton, G. Wilkinson, Advanced Inorganic Chemistry, Wiley-Interscience, New York, 1962.
[35] M.J. Torralvo, M.A. Alario, J. Soria, J. Catal. 86 (1984) 473.
[36] K. Haberko, A. Ciesla, A. Pron, Ceram. Int. 1 (1975) 111.
[37] E. Steger, G. Leukroth, Z. Anorg. Allg. Chem. 303 (1960) 169.